

# Accretion onto Binary YSOs through Gap from Their Circum-binary Disk

Tomoyuki Hanawa<sup>1,2</sup>, Yasuhiro Ochi<sup>2</sup> and Koichi Ando<sup>2</sup>

<sup>1</sup> Center for Frontier Science, Chiba University, Yayoi-cho 1-33, Chiba 263-8522, Japan [hanawa@cfs.chiba-u.ac.jp](mailto:hanawa@cfs.chiba-u.ac.jp)

<sup>2</sup> Graduate School of Science and Technology, Chiba University, Yayoi-cho 1-33, Chiba 263-8522, Japan

**Summary.** We have reexamined gas accretion onto YSO binary from the circum-binary disk on the basis of 2D numerical simulations with very high spatial resolution. The binary was assumed to have either a circular or an elliptic orbit. At the initial stage, the circum-binary disk has an inner edge at  $r_{\text{in}} \geq 1.75a$ , where  $a$  denotes the mean separation of the binary. The disk is assumed to rotate with the Keplerian velocity. We have confirmed that gas accretes from the circum-binary disk through the L<sub>2</sub> point into the Roche lobe. The gas accretes mainly onto the primary after circulating half around the secondary. This means that the accretion decreases the mass ratio. The accretion through gap is due to some pairs of two-armed spiral shock waves. While a pair of them corotates with the binary, the other pairs rotate more slowly, e.g., at  $\Omega = \Omega_*/4$  in most models, where  $\Omega_*$  denotes the mean angular velocity. Whenever the slowly rotating shock waves get across the L<sub>2</sub> point, the gas flow increases. Thus the accretion rate of the binary changes with the frequency,  $\nu = (3/2)(\Omega_*/2\pi)$ , in the case of a circular orbit. When the orbit is eccentric, the accretion rate changes mainly with the binary orbit but not purely periodically.

## 1 Introduction

Stars acquire their zero age masses mainly thorough accretion in the protostellar phase. Since majority of protostars have their companions, we should take account of the effects of their companions on the gas accretion. First, the gas accretion is shared between the primaries and secondaries in binaries. Second, the gravitational torque may induce gas accretion from the circum-binary disk in binaries. The former tends to lower the gas accretion, while the latter tends to enhance it. We have performed numerical simulations with extremely high spatial resolution to evaluate the two effects. From the numerical simulations we have found two new features. First, the accretion rate is highly oscillatory even when the binary orbit is circular. Second, the accretion rate on the primary is much larger than on the secondary. We show the results of our numerical simulations and discuss the implications.

## 2 Model and Method of Computation

We consider a binary system accreting gas from the circum-binary disk. We ignore the self-gravity of the accreting gas for simplicity. The binary is assumed to have either a circular or an eccentric orbit. We assume further that the binary and circum-binary disk are coplanar and hence the gas flow is two-dimensional for simplicity. The accreting gas is assumed to be isothermal. Then we solve the two-dimensional hydrodynamical equations,

$$\frac{\partial \Sigma}{\partial t} + \nabla \cdot (\Sigma \mathbf{v}) = 0, \quad (1)$$

and

$$\frac{\partial \mathbf{v}}{\partial t} + (\mathbf{v} \cdot \nabla) \mathbf{v} + c_s^2 \nabla \ln \Sigma + \nabla \Phi, \quad (2)$$

where  $\Sigma$ ,  $\mathbf{v}$ ,  $c_s$ , and  $\Phi$  denote the surface density of the gas, the gas velocity, the sound speed, and the gravitational potential, respectively. The gravitational potential is evaluated to be

$$\Phi(\mathbf{r}, t) = \Phi_1 + \Phi_2, \quad (3)$$

$$\Phi_i = \begin{cases} -\frac{GM_i}{|\mathbf{r} - \mathbf{r}_i|} & \text{for } |\mathbf{r} - \mathbf{r}_i| \geq R_i \\ -\frac{GM_i}{2R_i^3} (3R_i^2 - |\mathbf{r} - \mathbf{r}_i|^2) & \text{otherwise,} \end{cases} \quad (4)$$

where  $\mathbf{r}_i$  and  $R_i$  denote the position and the effective radius of each star, respectively. At the initial stage ( $t = 0$ ), the surface density is set to be

$$\Sigma_0 = 0.505 + 0.495 \tanh \left( \frac{r - r_{\text{in}}}{H} \right), \quad (5)$$

where  $r_{\text{in}}$  and  $H$  denote the radius of the disk inner edge and the width of the transition region. The initial velocity is set to be

$$\mathbf{v}_0 = \Omega \begin{pmatrix} -y \\ x \end{pmatrix}, \quad (6)$$

where

$$\Omega = \left[ \frac{G(M_1 + M_2)}{a^3} \min \left( 1, \frac{a^3}{r^2} \right) - \frac{c_s^2}{\Sigma_0 r} \frac{d\Sigma_0}{dr} \right]^{1/2}. \quad (7)$$

The density and velocity are kept at the initial values in the region  $r \geq r_{\text{out}}$ .

The hydrodynamical equations were integrated in the rotating frame of which angular velocity was the mean angular velocity of the binary. The computation region was covered with the Cartesian grid having  $2400^2$  to  $3456^2$  cells. We adopted the numerical scheme of Roe which captures shock waves without numerical oscillations. We used Monotone Upstream-centered Schemes for Conservation Laws (MUSCL) to achieve accuracy in time and space. The time step was taken to be twice longer in the region  $r \leq r_{\text{out}}/2$  than in the outer region. This dual time step reduced the numerical viscosity and hence improved the accuracy significantly.

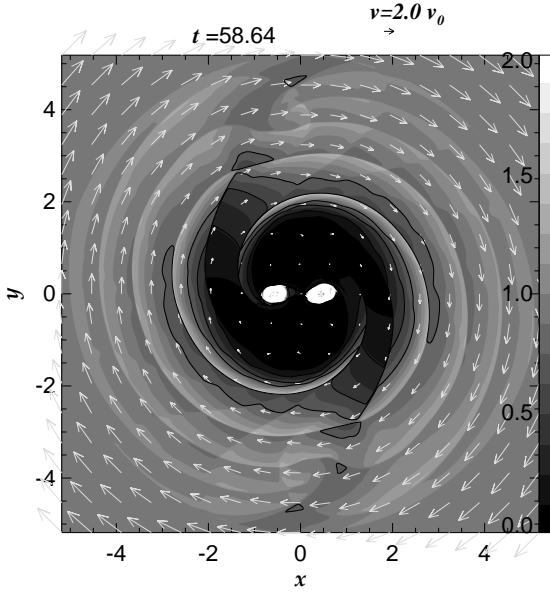


**Fig. 1.** The surface density distribution at the moment  $t = 58.64$  for the model with  $c_s = 0.2$ ,  $q = 0.8$ ,  $e = 0.0$ ,  $r_{\text{in}} = 1.75$ , and  $r_{\text{out}} = 5.175$  is shown. The arrows denote the velocity in the corotating frame.

### 3 Results

#### 3.1 Typical Model

Figure 1 shows the surface density distribution at  $t = 58.64$  for the model with  $c_s = 0.2$ ,  $q = 0.8$ ,  $e = 0.0$ ,  $r_{\text{in}} = 1.75$ , and  $r_{\text{out}} = 5.175$ . The brightness denotes the surface density in the linear scale in the surface density range  $\Sigma \leq 2$ . The circum-primary and circum-secondary disks have much higher surface densities. Although they are surrounded by a very low surface density region, the gas accretes from the circum-binary disk through the gap. The circum-binary disk has tightly wound spiral shock waves. While a pair of the spiral waves corotates with the binary, the other pair rotates more slowly. When the inner tail of the latter shock waves transit the  $L_2$  point, the accretion through the  $L_2$  point increases.

Figure 2 is the enlargement of the central part of Fig. 1. The circum-primary disk (right) has a higher surface density than the circum-secondary one (left). As shown by the arrows, the gas flows into the secondary lobe through the  $L_2$  point and into the primary lobe after circulating half around the secondary.

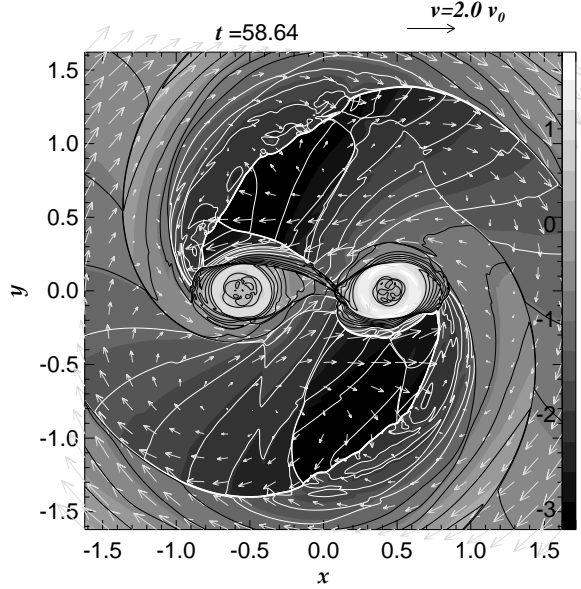


**Fig. 2.** The surface density distribution at the moment  $t = 58.64$  for the model with  $c_s = 0.2$ ,  $q = 0.8$ ,  $e = 0.0$ ,  $r_{\text{in}} = 1.75$ , and  $r_{\text{out}} = 5.175$  is shown. The arrows denote the velocity in the corotating frame.

Figure 3 shows the mass of the circum-primary disk,  $M_{1d}$ , and that of the circum-secondary one,  $M_{2d}$ , as a function of time. The former is defined as the mass contained in the circle the center of which coincides with the primary and with a radius equal to the distance from the primary to  $L_1$  point. The mass of the circum-secondary disk is defined similarly. The circum-primary disk is heavier than the circum-secondary disk, in contradiction with the earlier numerical simulations [1, 2].

Figure 4 shows the accretion rate of the circum-primary disk,  $\dot{M}_{1d}$ , oscillating with a large amplitude. The dashed curve denotes the average accretion rate,  $\langle \dot{M}_{1d} \rangle$ , which is obtained by fitting the 8th order polynomial to  $\dot{M}_{1d}$ . The average accretion rate has a peak around  $t = 28$  and decreases gradually. The average accretion rate of the circum-secondary disk is much lower than that of the circum-primary disk in the period  $t \geq 40$ , as shown in Fig. 3. We can evaluate the radial velocity in the circum-binary disk,

$$\langle v_r \rangle = -\frac{\dot{M}_{1d} + \dot{M}_{2d}}{2\pi\Sigma r}, \quad (8)$$

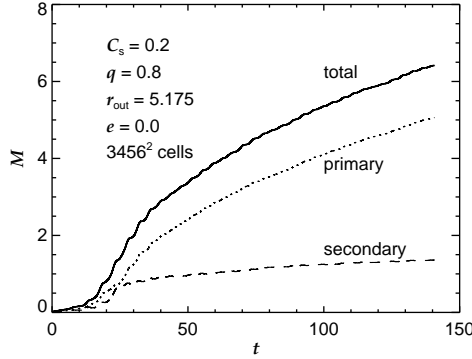


**Fig. 3.** The masses of the circum-primary (dashed) and circum-secondary (dotted) disks are shown as a function of the time for the model with  $c_s = 0.2$ ,  $q = 0.8$ , and  $e = 0$ . The solid curve denotes the sum of the disk masses.

$$\langle v_r \rangle = -4.0 \times 10^{-3} \left( \frac{M_1 + M_2}{0.05} \right) \left( \frac{r}{2a} \right)^{-1}, \quad (9)$$

from the average accretion rates. The evaluated radial velocity is much smaller than both the rotation velocity,  $v_\varphi$ , and the sound speed,  $c_s$ . It is even smaller than  $c_s^2/v_\varphi$ . This indicates that high accuracy is necessary for evaluating the accretion rate from the disk.

We computed the power spectrum of  $\dot{M}_{1d} - \langle \dot{M}_{1d} \rangle$  to evaluate the oscillation frequency of the accretion rate. The power spectrum has a main peak around  $2\pi\nu \simeq 0.75 \Omega_*$ , where  $\Omega_*$  denotes the angular velocity of the binary. Suppose that the oscillation frequency coincides with the synodic frequency between  $\Omega_*$  and  $\Omega_{sh}$ , where  $\Omega_{sh}$  denotes the pattern angular velocity of the shock wave. Then we have  $\Omega_{sh} \simeq 0.25 \Omega_*$ , since  $2\pi\nu = 0.75 (\Omega_* - \Omega_{sh})$ . This implies that the shock wave corotates with the circum-binary disk at  $r \approx 2.5a$  and is likely to be excited by some kind of 1:4 resonance. Remember that the Lindblad resonance has the angular velocity of  $\Omega_*/2$  and takes place at  $r = 1.59a$ . Thus the Lindblad resonance is not responsible for the excitation of the shock wave.

### 3.2 Dependences on Model Parameters

We have made more than 10 models by changing the spatial resolution and the model parameters  $q$ ,  $r_{in}$ ,  $r_{out}$ , and  $c_s$ . We have confirmed that the accretion rate on the circum-secondary disk is larger than that of the circum-primary disk when the spatial resolution is not sufficiently high [3]. The gas accretes directly onto the circum-secondary disk after inflowing through the  $L_2$  point when the spatial resolution is low. The direct accretion onto the circum-secondary disk is due to numerical viscosity. We think that the discrepancy

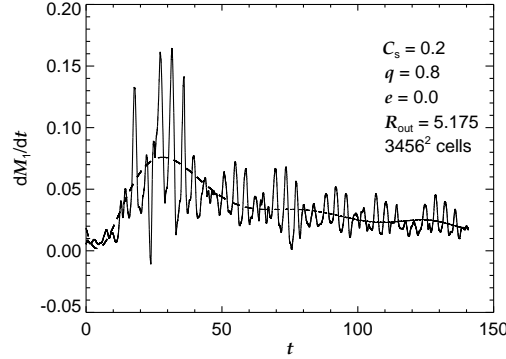


**Fig. 4.** The accretion rate on the circum-primary disk is shown as a function of the time for the model with  $c_s = 0.2$ ,  $q = 0.8$ , and  $e = 0$ . The dashed curve denotes the average accretion rate.

between the earlier simulations [1, 2] and ours is due to their low spatial resolution.

Qualitative features of our models depend little on the parameters  $q$ ,  $r_{\text{in}}$ ,  $r_{\text{out}}$ , and  $c_s$ . The differences between the models are mainly quantitative. When  $r_{\text{in}}$  is larger, the start of accretion is delayed. The delay is evaluated to be  $\Delta t = 25 \Delta r_{\text{in}}$  by comparing models with  $r_{\text{in}} = 1.75, 2.1$ , and  $2.5$ . This means that the disk's inner edge moves inward at  $v_{\text{in}} = -0.04$  – much faster than  $\langle v_r \rangle$  evaluated from the accretion rate. Thus the accretion from the circum-binary disk is mainly due to the angular momentum redistribution within the disk. The angular momentum redistribution is ascribed to spiral shock waves which are excited by resonance with the binary orbital motion.

When the binary orbit is eccentric, the power spectrum of the accretion rate has a peak at the rotation period,  $\nu = 1$ . The accretion rate changes not purely periodically but semi-regularly. The peak accretion rate differs from cycle to cycle. Again, the accretion rate of the circum-primary disk dominates over that of the circum-secondary disk.

## References

1. P. Artymowicz, S. H. Lubow: ApJ **467**, L77 (1996)
2. M. R. Bate, I. A. Bonnell: MNRAS **285**, 33 (1997)
3. Y. Ochi, K. Sugimoto, T. Hanawa: ApJ **623**, 922 (2005)